# 1

# Fundamental Properties of ZnO

*T. C. Collins and R. J. Hauenstein*
*Department of Physics, Oklahoma State University, Stillwater, OK, USA*

## 1.1 Introduction

### 1.1.1 Overview

Wurtzitic ZnO is a wide band gap semiconductor ($E_g = 3.437$ eV at 2 K) that has many applications, including piezoelectric transducers, varistors, phosphors, and transparent conduction films. Most of these applications only require polycrystalline materials; however, recent successes in producing large-area single crystals make possible the production of blue and UV light emitters and high temperature, high power transistors. The main advantage of ZnO as a light emitter is its large exciton binding energy ($E_b = 60$ meV). This binding energy is three times larger than that of the 20 meV exciton of GaN, which permits excitonic recombination to dominate in ZnO at room temperature (and even above). Excitonic recombination is preferable because the exciton, being an already bound system, radiatively recombines with high efficiency without requiring traps to localize carriers, as in the case in radiative recombination of electron–hole plasmas. Secondly, the deeper exciton of ZnO is more stable against field ionization due to piezoelectrically induced fields. Such piezoelectric effects are expected to increase with increasing dopant concentration for both ZnO and GaN.

For electronic applications, the attractiveness of ZnO lies in having high breakdown strength and high saturation velocity. ZnO also affords superior radiation hardness compared with other common semiconductor materials, such as Si, GaAs, CdS, and even GaN, enhancing the usefulness of ZnO for space applications. Optically pumped UV laser action in ZnO has already been demonstrated at both low and high temperatures

*Zinc Oxide Materials for Electronic and Optoelectronic Device Applications*, First Edition.
Edited by Cole W. Litton, Donald C. Reynolds and Thomas C. Collins.

although efficient electrically induced lasing awaits further improvements in the experimental ability to grow high quality p-type ZnO material. Nonetheless, over the past decade, researchers world-wide have made substantial theoretical and experimental progress concerning the p-type dopability of ZnO, with $10^{17}\,\text{cm}^{-3}$ range hole concentrations now plausibly achieved with material stability persisting for over 1 year, and with isolated (though often controversial) reports of hole concentrations as high as $\sim 10^{19}\,\text{cm}^{-3}$ even being reported from time to time. Finally, ZnO structures can be doped with transition metal (TM) ions to form dilute magnetic materials, denoted (Zn,TM)O, which can form a ferromagnetic state, an antiferromagnetic state as well as a general spin glass. The important point is that the Curie temperature ($T_C$) can be *above* room temperature. Such above-room-temperature anti- and ferromagnetic states form the basis for novel charge-based, spin-based, or even mixed spin- and charge-based devices which, collectively, are known as “spintronic” devices.

### 1.1.2 Organization of Chapter

The remainder of this chapter is organized as follows. In Section 1.2, a theoretical overview of the fundamental band structure of ZnO near the zone center is presented. The discussion includes the long-standing controversy over the symmetry-ordering of the valence bands at the Γ point. Next, in Section 1.3, the optical properties of intrinsic ZnO are reviewed, with particular emphasis on the excitons. Also presented in this same section are a discussion of the interaction of light, magnetic field, and strain field, as three examples of the general types of calculations done for excitons in ZnO, as well as a discussion of spatial resonance dispersion (Section 1.3.4) in which the polariton, a combined state arising out of the mixing of an exciton and light, plays a particularly important role. The electrical properties of ZnO are considered next in Section 1.4, including a discussion of intrinsic along with n-type and p-type ZnO. In particular, the important question of p-type dopability is discussed in detail in Section 1.4.3. For the implementation of optoelectronic devices, one will need Schottky barriers and ohmic contracts; recent progress in these areas is presented in Section 1.4.4. For heterojunction-based devices, band gap engineering will be required and this is considered in Section 1.5. Finally, presented in Section 1.6 is the theoretical basis for the ZnO spintronic device. The different models are based on the Heisenberg Spin Hamiltonian to describe the dilute magnetic system (Zn,TM)O. One can investigate both the interaction of the carriers with the magnetic moment of the TM as well as the TM–TM interactions. It is found that the resulting Curie temperature can be above room temperature. Spintronic devices made of (Zn,TM)O are expected to be faster and to consume less power since flipping the spin requires 10–50 times less power, and occurs roughly an order of magnitude faster, than does transporting an electron through the channel of traditional field-effect transistors (FETs).

## 1.2 Band Structure

### 1.2.1 Valence and Conduction Bands

The general electronic structure of binary III–V and II–VI compounds form semiconductors with the valence band mostly derived from the covalent bonding orbitals (s and p).

While the conduction band consists of antibonding orbitals, as one moves further outward from column IV of the periodic table, the binary compound semiconductors acquire a more ionic character. These compounds form cubic (zinc blende) and hexagonal (wurtzite) crystal structures, with ZnO crystallized in the wurtzite structure. The difference between the zinc blende and wurtzite structures is that the zinc blende is cubic while the wurtzite is a distortion of the cube in the [111] direction generally taken to be the z direction in the wurtzite.

The ionicity effect puts more electrons on the group V or group VI atoms giving the charge density more s and p characteristics of these elements in the valence band. It also causes gaps at the edge of the Brillouin zone compared with just covalent bonding materials. This translates into flatter bands across the Brillouin zone.

ZnO is a direct band gap semiconductor with valence-band maximum and conduction-band minimum occurring at the Γ point. The conduction band is s-like from Zn at Γ and is spin degenerate. The top three valence bands are p-like in character. They are split by the spin-orbit interaction in both the zinc blende and wurtzite symmetry, while wurtzite symmetry also has a crystal field splitting.

Figure 1.1 shows[1] the Quasi-cubic model[2–4] of the bottom of the con-duction band and the top of the valence band. Assuming that one has both zinc blende and wurtzite and that $\mathcal{H}_{\mathrm{so}} = \Delta \mathbf{L} \cdot \mathbf{S}$, one can write matrices of the form:

$$\begin{pmatrix} \Delta & 0 & 0 \\ 0 & \Delta & 0 \\ 0 & 0 & -2\Delta \end{pmatrix} \tag{1.1}$$

for zinc blende, using $j = 3/2$ and $j = 1/2$ eigenstates. For wurtzite the basis is rotated as stated above, so that one has $S_+\alpha$, $S_-\beta$, $-S_-\alpha$, $S_+\beta$, $S_z\alpha$, and $\mathrm{S}_z\beta$. This basis gives matrices (including crystal field effects $\delta$) of the form

$$\begin{pmatrix} \Delta & 0 & 0 \\ 0 & -\Delta & -i\sqrt{2}\Delta \\ 0 & i\sqrt{2}\Delta & -\delta \end{pmatrix}. \tag{1.2}$$

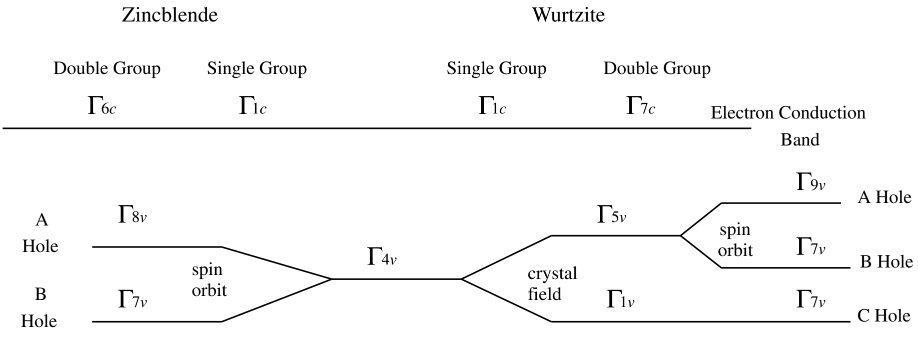

**Figure 1.1** *Structure and symmetries of the lowest conduction band and upmost valence bands in ZnO compounds at the Γ point*

Using the values obtained by Thomas,[5] a difficulty arises. As can be seen in Equation (1.3), there are values of energy difference which can give a complex number for $\delta$:

$$\delta = \frac{1}{2}(2E_1 + E_2) + \frac{1}{2}\sqrt{E_2^2 - 2E_1(E_1 + E_2)} \tag{1.3}$$

where $E_1$ is the energy difference between the $\Gamma_9$ excitons and $\Gamma_7$ exciton and $E_2$ is the energy difference between the two $\Gamma_7$ excitons. In fact, using Thomas[5] numbers, $\delta$ is a complex number with $\Gamma_9$ being the top valence band. This difficulty can be surmounted by assuming a negative spin-orbit splitting, which is different from all the other II–VI compounds and GaN. The physical mechanism that could produce a negative spin-orbit splitting was investigated by Cardona[6] for CuCl. In this zinc blende material, it was postulated that the valence band was formed from Cl wave functions, with a large proportion of Cu wave functions (Cu 4s3d). The inverted nature of the CuCl indicates that the Cu contributes a negative term to the spin-orbit splitting, since for this material the anion splitting is small and negative. Cardona6 estimated the "fraction" of the metal wave function in the valence band states by writing the spin-orbit splitting of the compound as:

$$\Delta = \frac{3}{2}[\alpha\Delta_{\mathrm{hal}} - (1-\alpha)\Delta_{\mathrm{met}}], \tag{1.4}$$

where $\alpha$ is the proportion of halogen in the wave function, $\Delta_{\mathrm{hal}}$ is the one-electron atomic spin-orbit splitting parameter of the halogen and $\Delta_{\mathrm{met}}$ is one of the d-electrons of the metal. This gave $\alpha = 0.25$ for CuCl. It was also presented that the energy interval between the ground state of the $Cu^+$ ion ($3d^{10}$) and the first excited state ($3d^9$, 4s) is 2.75 eV.

Returning to ZnO, one finds the Zn d-bands below the uppermost p-like valence bands to be greater than 7 eV.[7–9] This makes it very unlikely that one has much mixing at all. Further, the d-band appeared to be relatively flat, noting again very little mixing. Also, the availability of ZnO crystals in which intrinsic exciton transitions[10] are observed in emission and their splitting in a magnetic field have led to a positive spin-orbit splitting of 16 meV. With this interpretation, the Quasi-cubic model[2–4] gives results in line with the other II–VI compounds.

In order to investigate the valence band ordering of ZnO further, Lambrecht *et al.*[11] calculated the band structure of ZnO using a linear muffin-tin potential and a Kohn–Sham local density approximation. The band gap at $\Gamma$ was 1.8 eV compared with experiment of 3.4 eV and the Zn d-band was approximately 5 eV below the top of the valence band at $\Gamma$. To correct for the band gap Reynolds *et al.*[10] rigidly shifted the conduction band up to match the experimental $\Gamma$-point gap (a shift of 1.624 eV).

As is seen from above in the Quasi-cubic model,[2–4] the spin-orbit magnitude and sign are a function of the energy difference between the top of the valence and the 3d band of Zn. It is found to be greater than 7 eV.[7–9] In Reynolds *et al.*,[10] the d-band was adjusted to where the spin-orbit gave the right energy difference with the $\Gamma_7$ above the $\Gamma_9$. The d band was put at 6.25 eV below the top of the valence band. This led to a negative *g*-value and of course a negative spin-orbit parameter. This in turn matched the experimental data given in Hong *et al.*[9] but with a different interpretation of the splitting of the exciton lines. Thus, there is no agreement of the spin-orbit value for ZnO. In first principle electron structure calculations, one has an accuracy only on the order of ~100 meV whereas the splittings of the levels in the top valence band are on the order of ~10 meV!

## 1.3 Optical Properties

### 1.3.1 Free and Bound Excitons

The optical absorption (emission) of electromagnetic radiation in a ZnO crystal is dependent on the matrix element

$$\int \Psi_f^* \mathcal{H}_{\text{int}} \Psi_i d\tau \tag{1.5}$$

where

$$\mathcal{H}_{\text{int}} = \frac{e\hbar}{imc} \mathbf{A} \cdot \nabla. \tag{1.6}$$

Here, $\mathbf{A}$ is the vector potential of the radiation field and has the form

$$\mathbf{A} = \hat{n}|\mathbf{A}_0|e^{i(\mathbf{q}\cdot\mathbf{r}-\omega t)},$$

$e$ is the electronic charge, $m$ is the electron mass, $c$ is the velocity of light, $\hat{n}$ is a unit vector in the direction of polarization, and $\mathbf{q}$ is the wave vector. Expanding the spatial part of $\mathbf{A}$ in a series gives

$$\mathcal{H}_{\text{int}} \equiv \sum_{j=0}^{\infty} \mathcal{H}_{\text{int}}^j \tag{1.7}$$

where

$$\mathcal{H}_{\text{int}}^j = (\mathbf{q}\cdot\mathbf{r})^j \hat{n}\cdot\nabla \tag{1.8}$$

and the dipole term is then the first term ($i = 0$). The matrix element in Equation (1.5) transforms under rotation like the triple direct product

$$\Gamma_f \otimes \Gamma_r^j \otimes \Gamma_i. \tag{1.9}$$

The selection rules are then determined by which of the triple-direct-product matrix elements in question do not vanish, where $\Gamma_r^j$ is the symmetry of the expansion term $\mathcal{H}_{\text{int}}^j$ in Equation (1.8).

The dipole moment operator for electric dipole radiation transforms like $x$, $y$, or $z$ dependent on the polarization. When the electric field vector $\mathbf{E}$ of the incident light is parallel to the crystal axis of ZnO, the operator corresponds to the $\Gamma_1$ representation. When it is perpendicular to the crystal axis, the operator corresponds to the $\Gamma_5$ representation. Since the crystal has a principal axis, the crystal field removes part of the degeneracy of the p-levels as seen in Figure 1.1. Including spin in the problem doubles the number of levels. Since the conduction band at $\mathbf{k} = 0$ is the Zn (4s) level[4,5] it transforms as $\Gamma_7$ while the $\mathbf{k} = 0$ at top of the valence band is made up of the O(2p) level and it splits into (p$_x$, p$_y$)Γ5 and ($p_z$)Γ1. When crossed with the spin one has

$$\Gamma_5 \otimes D_{1/2} \rightarrow \Gamma_7 + \Gamma_9 \tag{1.10}$$

$$\Gamma_1 \otimes D_{1/2} \rightarrow \Gamma_7 \tag{1.11}$$

as shown in Figure 1.1.

One of the light absorption (emission) intrinsic states is an exciton, which is made up of a hole from the top of the valence band and an electron from the bottom of the conduction band. These are excitations of the $N$-particle system whereas electron structure calculations are of the ($N \pm 1$)-particle system. All solutions to the one-body calculations such as the one-particle Green's functions method do not contain the interaction of the excited "particle" with the other "particles." The more localized the excitation the more important it is to include this interaction. The more localized the excitation is, the flatter the one-electron bands, leading to heavier effective masses. This is turn leads to increased binding energy of the electron–hole pair. In ZnO, the binding energy of the ground state exciton is 60 meV. Adding in the Coulomb term of the electron–hole pair gives a hydrogenically bound pair. For the $\Gamma_9$ hole and $\Gamma_7$ electron one has

$$\Gamma_9 \otimes \Gamma_7 \rightarrow \Gamma_5 + \Gamma_6, \tag{1.12}$$

and for the $\Gamma_7$ hole and $\Gamma_7$ electron one has

$$\Gamma_7 \otimes \Gamma_7 \rightarrow \Gamma_5 + \Gamma_1 + \Gamma_2. \tag{1.13}$$

The $\Gamma_5$ and $\Gamma_6$ are doubly degenerate and the $\Gamma_1$ and $\Gamma_2$ are nondegenerate. The Hamiltonian for the exciton becomes:

$$\mathcal{H} = \mathcal{H}_e + \mathcal{H}_h + \mathcal{H}_{\text{int}}, \tag{1.14}$$

where $\mathcal{H}_e$ and $\mathcal{H}_h$ are the Hamiltonian for the electron and the hole and $\mathcal{H}_{\text{int}}$ is the interaction between the electron and hole including Coulomb, exchange and correlation. To first approximation one generally includes just the Coulomb term as noted above. Equation (1.14) gives what are referred to as the "free" excitons.

There are several extrinsic effects which modify the excitons. Most notable of these in ZnO are the bound complexes. One can have the exciton bound to an ionized donor or a neutral donor. In the case of the ionized donor, one has the molecular attraction of the exciton to the donor plus central cell corrections. For the neutral donor, one has again the molecular binding energy plus the ability of the neutral donor to be left in an excited state. Similar results are obtained with the ionized acceptor or neutral acceptor. The method of calculating these systems is to treat the system as a molecular system in the field of the crystal.

### 1.3.2 Effects of External Magnetic Field on ZnO Excitons

The case of an applied uniform magnetic field was developed by Wheeler and Dimmock[12] for the exciton in ZnO. It was assumed the electron bands are isotropic at least to second order in **k** with only double spin degeneracy. The exciton equation is a simple hydrogen Schrödinger equation including effective-mass and dielectric anisotropies. It is found that the mass anisotropy is small, allowing first-order perturbation calculations to be made for the energy states as well as for the magnetic-field effects.

Since the valence and conduction band extrema are at $\mathbf{k} = 0$, the wave vector of the light that creates the exciton $\mathbf{k}$ will also represent the position of the exciton in $\mathbf{k}$-space. Dividing the momentum and spaces coordinates into the center-of-mass coordinates and the internal coordinates, the exciton Hamiltonian can be divided into seven terms as follows:

$$\mathcal{H} = \mathcal{H}_1 + \mathcal{H}_2 + \mathcal{H}_3 + \mathcal{H}_4 + \mathcal{H}_{k1} + \mathcal{H}_{k2} + \mathcal{H}_{k3} \tag{1.15}$$

$$\mathcal{H}_1 = -\frac{\hbar^2}{2m}\left[\frac{1}{\mu_x}\left(\frac{\partial^2}{\partial x^2} + \frac{\partial^2}{\partial y^2}\right) + \frac{1}{\mu_z}\frac{\partial^2}{\partial z^2}\right] - \frac{e^2}{\epsilon\eta^{1/2}}\left(x^2 + y^2 + \eta^{-1}z^2\right)^{-1/2} \tag{1.16}$$

$$\mathcal{H}_2 = -2i\zeta\left(\frac{A_x}{\Delta_x}\frac{\partial}{\partial x} + \frac{A_y}{\Delta_y}\frac{\partial}{\partial y} + \frac{A_z}{\Delta_z}\frac{\partial}{\partial z}\right) \tag{1.17}$$

$$\mathcal{H}_3 = \frac{e}{2mc^2}\left(\frac{A_x^2}{\mu_x} + \frac{A_y^2}{\mu_y} + \frac{A_z^2}{\mu_z}\right) \tag{1.18}$$

$$\mathcal{H}_4 = \frac{\zeta}{2}\sum_{i=x,y,z}\left(g_{e_i}S_{e_i} + g_{h_i}S_{h_i}\right)H_i \tag{1.19}$$

$$\mathcal{H}_{k1} = \frac{-i\hbar}{2m}\left(\frac{K_x}{\Delta_x}\frac{\partial}{\partial X} + \frac{K_y}{\Delta_y}\frac{\partial}{\partial Y} + \frac{K_z}{\Delta_z}\frac{\partial}{\partial Z}\right) \tag{1.20}$$

$$\mathcal{H}_{k2} = \zeta\left(\frac{K_x}{\mu_x}A_x + \frac{K_y}{\mu_y}A_y + \frac{K_z}{\mu_z}A_z\right) \tag{1.21}$$

$$\mathcal{H}_{k3} = \frac{\hbar^2}{8m}\left(\frac{K_x^2}{\mu_x} + \frac{K_y^2}{\mu_y} + \frac{K_z^2}{\mu_z}\right), \tag{1.22}$$

where $m$ is the free-electron mass and $\mu_x$ is the reduced effective mass of the exciton in the $x$ direction at $\Gamma$ ($\mu_x = \mu_y$). Also,

$$\zeta = \frac{e\hbar}{2mc} \qquad \eta = \frac{\epsilon_z}{\epsilon_x} \tag{1.23}$$

$$\mathbf{A} = \frac{1}{2}(\mathbf{H} \times \mathbf{r}) \tag{1.24}$$

$$\frac{1}{\Delta_y} = \left(\frac{m}{m^*_{ey}} - \frac{m}{m^*_{hy}}\right). \tag{1.25}$$

The first term is the Hamiltonian for a hydrogenic system in the absence of external fields. One could include the possibility of the mass and dielectric anisotropies. The second term is an **A**·**p** term which leads to the linear Zeeman magnetic field term. In this term, the momentum operator is $\mathbf{p}_i - 2e\,\mathbf{A}_i/c$ where $\mathbf{A}_i = (1/2)\mathbf{H} \times \mathbf{r}_i$ is the vector potential, **H** is the magnetic field, and $\mathbf{r}_i$ is the coordinate of the *i*th electron. The $A^2$ term is the diamagnetic field term proportional to $|H|^2$. The fourth term is the linear interaction of the magnetic field with the spin of the electron and hole. If one has small effective reduced mass for the electron and a large dielectric constant, the radii of the exciton states are much larger than the corresponding hydrogen-state radii. Hence, the spin-orbit coupling is proportional to $r^{-3}$ and thus quite small, it is legitimate to write the magnetic field perturbations in the Paschen–Back limit as done above.

The last three terms are the **K**·**P**, **K**·**A**, and $K^2$ terms; **K** is the center-of mass momentum. Treating the **K**·**P** to second order and adding the $K^2$ term, one can obtain an energy term that appears like the center-of-mass kinetic energy. The **K**·**A** term has little effect upon the energy; however, it has very interesting properties. This term represents the quasi-electric field that an observer riding with the center-of-mass of the exciton would experience because of the magnetic field in the laboratory. This quasi-field would produce a Stark effect linear in **H**, and this would give rise to a maximum splitting interpretable as a "*g*" value.

### 1.3.3 Strain Field

The effective Hamiltonian formalism of Pikus[13,14] is of the form

$$\mathcal{H} = \mathcal{H}_{v-0} + \mathcal{H}_{v-p} + \mathcal{H}_c + \mathcal{H}_{\text{int}}, \tag{1.26}$$

Using the angular momentum operators $J(L = 1)$ gives

$$\mathcal{H}_{v-0} = \Delta_1 J_z^2 + \Delta_2 J_z \sigma_z + \Delta_3(\sigma_+ J_- + \sigma_- J_+), \tag{1.27}$$

where $\Delta_1$ is the crystal field splitting of the $S_x$, $S_y$ bands from the $S_z$ band; $\Delta_2$ is the spin-orbit splitting of the $j = 3/2$ bands from the $j = 1/2$ band, and $\Delta_3$ is a trigonal splitting of the $|j, m_j\rangle = |\frac{3}{2}, \pm\frac{3}{2}\rangle$ bands from the $|\frac{3}{2}, \pm\frac{1}{2}\rangle$ bands.

The operator $\mathcal{H}_{v-\mathrm{p}}$, which describes the interaction between the valence bands due to strain, can be determined from symmetry considerations by combining the strain tensor $\varepsilon_{ij}$ with the angular momentum operators $J$ and $\sigma$:

$$\begin{aligned}\mathcal{H}_{v-p} &= (C_1 + C_3 J_z^2)\varepsilon_{zz} + (C_2 + C_4 J_Z^2)(\varepsilon_{xx} + \varepsilon_{yy}) \\ &\quad + C_5(J_-^2 \varepsilon_+ + J_+^2 \varepsilon_-) + C_6([J_z J_+]\varepsilon_{-z} + [J_z J_-]\varepsilon_{+z})\end{aligned} \tag{1.28}$$

Here,

$$\varepsilon_{\pm} = \varepsilon_{xx} - \varepsilon_{yy} \pm 2i\varepsilon_{xy} \quad \varepsilon_{\pm z} = \varepsilon_{xz} \pm i\varepsilon_{yz}, \tag{1.29}$$

and $[J_iJ_j] = (J_iJ_j + J_jJ_i)/2$. These operators then describe the mixing of the p-like valence bands due to crystalline strain in the terms of material-dependent parameters (the $C_i$'s).

The operator $\mathcal{H}_c$ represents the conduction-band energy. Because of the $\Gamma_1$ symmetry of the conduction band, the operator has the form

$$\mathcal{H}_c = E_c + d_1\varepsilon_{zz} + d_2(\varepsilon_{xx} + \varepsilon_{xy}). \tag{1.30}$$

$\mathcal{H}_{\text{int}}$ is the Coulomb interaction plus the exchange term

$$\mathcal{H}_{\text{int}} = E_b + \frac{1}{2}j\sigma_h \cdot \sigma_e \tag{1.31}$$

where in Equation (1.31)$j$ denotes the usual exchange integral (not to be confused with the usage of $j$ as the angular momentum quantum number in the earlier equations). The exchange term has off-diagonal matrix elements, and for example, removes the $\Gamma_5$ degeneracy. This leads to strain splittings, which are measured.

### 1.3.4 Spatial Resonance Dispersion

The excitons in ZnO interact with photons when the wave vector are essentially equal. The energy denominator for exciton–photon mixing is small and the mixing becomes large. These states are not to be considered as pure photon states or pure exciton states, but rather mixed states. Such a mixed state is called a polariton. When there is a dispersion of the dielectric constant, spatial dispersion has been invoked to explain certain optical effects of the crystal. This causes more than one energy transport mechanism. Spatial dispersion addresses the possibility that two different kinds of waves of the same energy and same polarization can exist in a crystal differing only in wave vector. The one with an anomalously large wave vector is an anomalous wave. In the treatment of dispersion by exciton theory, it was shown that if the normal modes of the system were allowed to depend on the wave vector, a much higher-order equation for the index of refraction would result. These new solutions occur whenever there is any curvature of the ordinary exciton band in the region of large exciton–photon coupling. These results apply to the Lorentz model as well as to quantum-mechanical models whenever there is a dependence of frequency on wave vector.

The specific dipole moment of polarization of a crystal and the electric field intensity are not in direct proportion. The two are related by a differential equation that resulted in giving Maxwell equations of higher order. This leads to the existence of several waves of the same frequency, polarization, and direction but with different indices of refraction. The index of refraction becomes

$$n^2 = \frac{k^2c^2}{\omega^2} = \epsilon + \sum_j \frac{4\pi(a_{0j} + a_{2j}K^2)\omega_{0j}^2}{\omega_{0j}^2 + (\hbar\omega_{0j}k^2/m^* - \omega^2 - i\omega\Gamma)}. \tag{1.32}$$

Here, the sum over $j$ is to include the excitons in the frequency region of interest, and the contributions from other oscillators are included in a background dielectric constant $\epsilon$. In Equation (1.32) the numerator and denominator have been expanded in powers of $k$, keeping terms to order of $k^2$, $m^*$ is the sum of the effective masses of the hole and electron that comprise the exciton, and $\omega_{0j}$ is the frequency of the $j^{\text{th}}$ oscillator at $\mathbf{k}=0$. Eliminating $k^2$ from Equation (1.32) and neglecting the linewidth of the oscillators, the equation becomes

$$n^2=\epsilon+\sum_j \frac{4\pi(a_{0j}+a_{2j}\omega^2 n^2/c^2)\omega_{0j}^2}{\omega_{0j}^2+(\hbar\omega_{0j}\omega^2 n^2/c^2 m^*)-\omega^2}. \tag{1.33}$$

The sum is over excitons from the top two valence bands where the "allowed" excitons have been included with $a_{0j}\neq 0$, $a_{2j}=0$ while the "forbidden" (because excitons are included with $a_{0j}\neq 0$, $a_{2j}=0$). Equation (1.33) reduces to a polynomial in $n^2$ whose roots give the wavelengths of the various "normal modes" for the transfer of energy within the crystal.

There is another structure seen in the spectra near the free exciton. This is the result of the mixing of the exciton and photon with non crossing effects of the photon dispersion. This creates a larger density of states where the mixing becomes strong enough to bind the photon curve.

## 1.4 Electrical Properties

Electrically, ZnO is a transparent-conducting-oxide semiconductor which at room temperature exhibits defect- or impurity-dominated n-type conductivity, even in nominally undoped materials. This defect- or impurity-dominated conductivity is a consequence of the large band gap[15,16] (≈3.3 eV at room temperature) combined with the unavoidable presence of electrically active native defects and impurities with donor ionization energies typically[15] ~10–100 meV at concentrations typically[15] $\sim 10^{15}$–$10^{16}\,\text{cm}^{-3}$. Furthermore, while ZnO is readily doped n-type and carrier concentrations as high as $\sim 10^{21}\,\text{cm}^{-3}$ are achievable,[17] at present p-type doping remains challenging. Furthermore, for purposes of utilizing ZnO-based materials for extending semiconductor optoelectronics further into the UV, two of the biggest technological challenges will be to develop growth and device-processing techniques to achieve control over p-type doping as well over metal/semiconductor junction formation (including both Schottky and ohmic contacts) to both n-type and p-type materials.

Most of what is known experimentally about the electronic properties of "pure" ZnO is actually based on n-type specimens. The fundamental electronic transport properties of nominally undoped and intentionally doped ZnO will be presented in Section 1.4.1. Next, in Section 1.4.2, intentional n-type doping and dopants will be considered. Then, in Section 1.4.3 will be discussed recent progress, both experimental and theoretical, concerning the technologically important question of p-type dopability in ZnO. Finally, recent progress on the fabrication of Schottky contacts to n-type, and of ohmic contacts to both n-type and p-type ZnO, will be reviewed in Section 1.4.4.

### 1.4.1 Intrinsic Electronic Transport Properties

To date, available data concerning fundamental electronic properties of intrinsic, accurately stoichiometric ZnO remains largely unknown.[15] In part this is because of the historical unattainability of sufficiently high-quality materials, a consequence of the difficulty (especially through bulk crystal-growth methods) in achieving adequate O incorporation into the specimen. While such a circumstance may seem merely a technological rather than a fundamental limitation, recent theoretical work[18,19] suggests that the n-type character resulting from electrically active stoichiometric native point defects such as vacancies, inter-stitials, and antisites,[18] as well as the unusually nonamphoteric and donor-like character of unintentional but ever-present hydrogen,[20] may be inherent to ZnO, at least, to materials produced through the use of near-equilibrium crystal growth methods. The question of p-type dopability shall be deferred to Section 1.4.3. For the remainder of the present section we will consider the basic electronic transport properties of nominally undoped ZnO which have been established experimentally, along with modifications due to intentional n-type doping.

In general, electrical transport properties of ZnO are directionally dependent due to the anisotropy of its wurtzite crystal structure. For the case of nominally undoped (i.e. residually n-type $\sim 10^{16}\,\mathrm{cm}^{-3}$ carrier concentration) ZnO, Figure 1.2 shows temperature-dependent Hall mobility data for current transport both parallel and perpendicular to the crystallographic c axis of bulk ZnO. As seen in Figure 1.2, the electron mobility attains a peak value of $\sim 1000\,\mathrm{cm}^2\,\mathrm{V}^{-1}\,\mathrm{s}^{-1}$ at a temperature of 50–60 K, and drops off approximately as the power law, $T^p$ for low temperatures and $T^q$ for high temperatures where $p \approx 3$ and $q \approx -2$ in Figure 1.2(a). The drop off at low temperature falls off faster than that expected due to ionized-impurity scattering alone whereas that at high temperatures is attributable primarily to the combination of acoustic-deformation-potential with polar-optical-phonon scattering mechanisms.[21] The slight anisotropy observed in Hall mobility data [compare Figure 1.2(a) and (b)] has been attributed exclusively to piezoelectric scattering.[15]

Also of interest is the electric-field dependence of the mobility. Figure 1.3 compares theoretically obtained plots[22] of drift velocity ($v_d$) vs electric field; results predicted for ZnO are contrasted with those for GaN, another direct-gap semiconductor having a closely comparable band gap ($E_g^{\mathrm{GaN}} \approx 3.4\,\mathrm{eV}$) to ZnO. A comparison of the GaN and ZnO curves at low field reveals that $\mu_{\mathrm{ZnO}} < \mu_{\mathrm{GaN}}$ while at the same time the saturated drift velocities obey the opposite relation: $\upsilon_{\mathrm{Sat}}^{\mathrm{ZnO}} > \upsilon_{\mathrm{Sat}}^{\mathrm{GaN}}$. For hot-electron devices, where fields are high and transport is nonohmic, it is $\upsilon_{\mathrm{sat}}$ rather than $\mu$ that can be the more important parameter to device operation.[23]

## 1.4.2 n-type Doping and Donor Levels

Intentional n-type doping is readily achieved through the use of column-III elements such as Al, Ga, or In, or, column-VII elements such as Cl, F, or I. All of these sit substitutionally on the appropriate cation or anion site and form reasonably shallow levels. In a 2001 review article, Look discusses the presence of three predominant donor levels in ZnO appearing at approximately 30, 60, and 340 meV.[23] Among these, the 60 meV level is that corresponding to effective mass theory (≈65 meV), whereas the 30 meV level was at the time believed[18,24] to be due to interstitial Zn ($\mathrm{Zn_i}$) and no longer believed to be due to the O vacancy ($\mathrm{V_O}$), which instead was thought to be a deep donor.[18] The identity of the 340 meV level was not established. Interestingly, also presented by Look in this same review article[23] are some of his own temperature-dependent Hall mobility data which

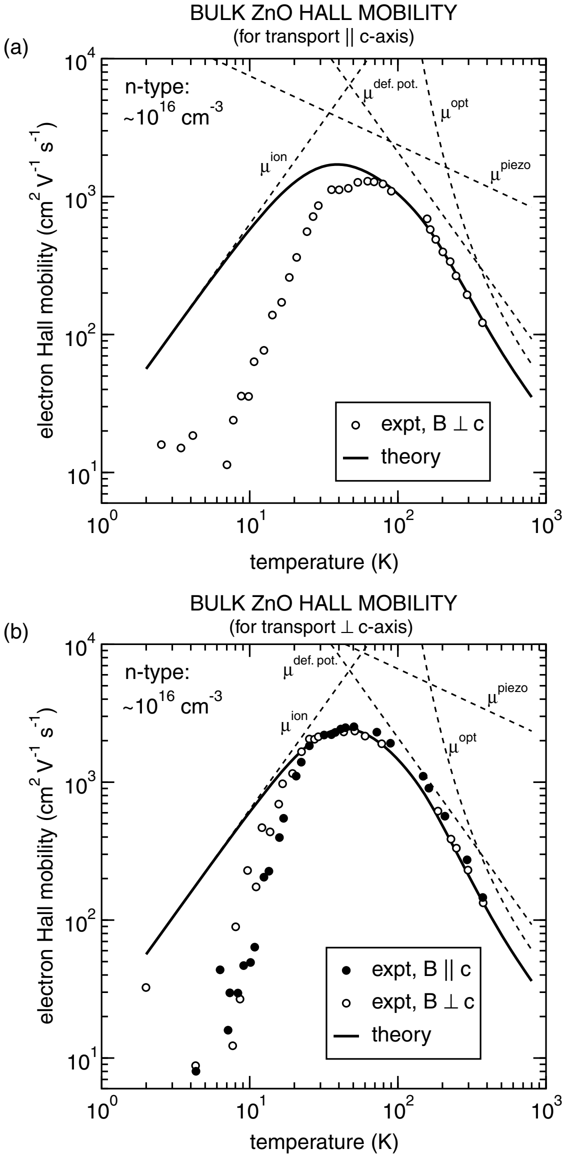

***Figure 1.2*** *Hall mobility vs temperature of nominally undoped ZnO. Current transport is parallel in (a) and perpendicular in (b) to the wurtzite c-axis. In each case, the magnetic field is perpendicular to the current flow. Superimposed are theoretical curves corresponding to separate scattering mechanisms. Reprinted from R. Helbig, P. Wagner, Halleffekt und anisotropie der beweglichkeit der elektronen in ZnO,. Phys. Chem. Solids 35, 327. Copyright (1974) with permission from Elsevier*

were at the time obtained on single crystals grown through the use of relatively modern bulk techniques such as the seeded vapor phase transport (SVPT) method. The SVPT-grown sample in this case was seen to exhibit a temperature-dependent mobility which compares very favorably to the best results from the older literature (shown in Figure 1.2),

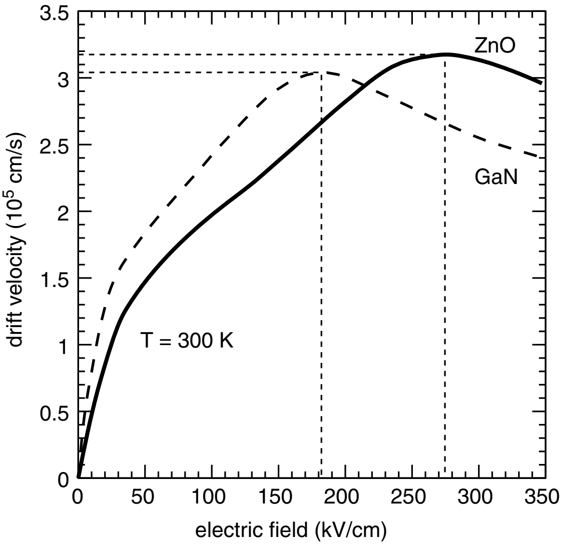

*Figure 1.3 Theoretical electron drift velocity vs electric field for ZnO (solid line) and GaN (dashed line). Though GaN exhibits higher mobility at low fields, ZnO is expected to have greater saturated drift velocity at high fields. Reprinted from J. D. Albrecht, et al., High field electron transport properties of bulk ZnO. J. Appl. Phys. 86, 6864. Copyright (1999) with permission from American Institute of Physics*

with peak mobility of $\approx 1900\,\text{cm}^2\,\text{V}^{-1}\,\text{s}^{-1}$, once again occurring near 60 K.[23] Analysis of the temperature-dependent mobility data[23] indicates for this sample the presence of the two shallow donors mentioned above (31 and 61 meV at donor concentrations of $9 \times 10^{15}$ and $1 \times 10^{17}\,\text{cm}^{-3}$, respectively) along with a shallow acceptor level ($N_A = 2 \times 10^{15}\,\text{cm}^{-3}$; $E_A$ not given).[23]

In addition to the list of above-mentioned substitutional n-type species may be added interstitial H which, while normally entering as an amphoteric species for most other semiconductors (either as $H^+$ or $H^-$ as needed to effect passi-vation), for ZnO enters only in the positive charge state, and thus is able to contribute to doping rather than passivation through the formation of a O–H complex, according to a recent theoretical prediction by Van de Walle.[20] This atypical behavior of H when in ZnO is attributed to the strong O–H bond which forms and functions as an effective donor "atom" sitting on an O site.[20] As an aside, it is interesting to observe that the long-standing p-type-dopability problem in GaN was finally resolved once it was realized that, in that case, H acts as a passivating agent (through formation of complexes with the intended acceptor species). Evidently, though the roles played by H in ZnO and GaN appear to be entirely different, it would appear nonetheless important to minimize the H concentration for purposes of achieving p-type material.

### 1.4.3 p-type Doping and Dopability

For ZnO to be technologically successful as a UV-range optoelectronic device material, an important growth issue is the ability to reliably produce both n-type and p-type ZnO materials. As noted above, n-type doping is readily achieved (and occurs natively through $Zn_i$ and possibly other defects in stoichiometry). However, like most wide-band-gap semiconductors, including other II–VI compounds[25] as well as III–V refractory-nitride compounds AlN (presently) and GaN (previously), ZnO exhibits an asymmetric ease of dopability one way (n-type) but not the other way (p-type). The physical origins of such dopability asymmetries in the II–VIs generally have been reviewed recently by Desnica;[25] briefly, doping-limiting mechanisms common to II–VI semiconductors include self-compensation (via native defects, lattice relaxation, amphoteric incorporation), solubility limitations, activation-efficiency limitations, in addition to other mechanisms which do not apply to higher hardness materials such as ZnO.[25]

Prior to 1999 there was only one report[26] of p-ZnO and in that case both material quality and growth reproducibility were poor. Since that time have come a number of papers, at first mostly theoretical, and more recently experimental, seeking to elucidate or obviate the difficulties of ZnO p-type doping. Among the conclusions from the aforementioned body of theoretical work[18–20,27,28] –all since 1998 and all based on *ab initio* band calculations–are the following explanations and conclusions concerning the long-standing p-type-doping problem in ZnO and how it might be solved.

According to Yamamoto and Katayama-Yoshida,[27] the doping asymmetry of ZnO is the consequence of fundamentally opposing effects of doping type on Madelung energy [n-type (p-type) doping decreases (increases) the Madelung energy]. If this is the governing mechanism, then, the proper strategy to attain p-ZnO should be to co-dope with both donors and acceptors, for example, p-ZnO:(N,Ga).

An alternative explanation was put forth by Zhang *et al.*[18] who considered the case of intrinsic ZnO and examined through *ab initio* theory the energetics of formation of native point defects as well as the donor or acceptor level(s) that these defects introduce. For each type of native stoichiometric point defect (e.g. $Zn_i$, $Zn_O$, $V_O$, which are all the possible native donors in ZnO, and $O_i$ and $V_{Zn}$ which are all the acceptors) they systematically computed, for each defect, its formation enthalpy and any donor or acceptor level(s) which it intro-duced. They concluded that native ZnO should only be able to come out n-type but never p-type, assuming growth under quasi-equilibrium conditions.[18] The argument could be stated as follows: Under Zn-rich growth conditions, $Zn_i$, a shallow donor, should form readily due to favorable thermodynamics, and the only possible compensators ($O_i$, $V_{Zn}$) both have unfavorable thermodynamics for formation. Thus, the prediction is that nominally undoped ZnO grown under Zn-rich conditions (again through equilibrium techniques) should come out n-type due to the existence of uncompensated $Zn_i$ donor defects. Equally, under either O-rich or Zn-rich conditions: natively p-type ZnO should not be possible because there always should be some native donor defect ($V_O$, $Zn_i$, or $Zn_O$) which–shallow or deep–would be favored to form thermodynamically (which one forms would depend upon the growth conditions), and hence should be available to compensate any possible native acceptor defects ($O_i$, $V_{Zn}$) which might have formed.[18] However, it is important to note that this theory specifically presupposes equilibrium (quasi-equilibrium) crystal growth; thus, it might be theoretically possible in principle through nonequilibrium techniques to "freeze in" a metastable p-ZnO film though, evidently, the origin of the acceptor would probably have to be an impurity species rather than a native point defect of ZnO.

In another *ab initio* study, this time for extrinsic ZnO, Yan *et al.*[28] considered the role of the impurity species chemical potential in addition to those of the host (Zn and O) species considered in the earlier work by Zhang *et al.*[18] just discussed. Yan *et al.*'s work predicts that through consideration together of both dopant (N) and host (O in particular) chemical potentials during equilibrium growth that the use of certain N-containing dopant species–either NO or $NO_2$ in particular (as opposed to the $N_2$ or $N_2O$ that had been actually attempted initially but with little success)–should enable p-type doping. It is noteworthy that both Yan *et al.*'s and Zhang *et al.*'s theories provide alternative explanations to the "co-doping" concept as proposed by Yamamoto and indeed show the latter to be incorrect. Finally, in a later theoretical overview, Zunger[29] summarized on general grounds the thermodynamics of dopant incorporation ("dopant" in this context referring either to an impurity or to a native defect often spontaneously formed) by way of the formation enthalpy $\Delta H^{(\mathrm{D},q)}$ for an arbitrary dopant D in a host crystal wherein the dopant is formed in charge state $q$ ($q > 0$ for donors and $q < 0$ for acceptors):

$$\Delta H^{(D,q)}(\mu, \varepsilon_F) = q\varepsilon_F + n_D(\mu_D - \mu_H)\Delta U_b. \tag{1.34}$$

In this equation, $\varepsilon_\mathrm{F}$ is the Fermi energy, $\mu_{\mathrm{D,H}}$ are the chemical potentials of dopant and host, respectively, and $\Delta U_\mathrm{b}$ denotes any excess energy associated with local chemical bonds around the dopant, relative to the otherwise undoped crystal. The $q\varepsilon_\mathrm{F}$ term of Equation (1.34) explains the thermodynamic origin of the spontaneous formation of so-called "killer defects". For example, if one were to attempt to dope ZnO p-type via a near-equilibrium crystal-growth technique, the lowering of $\varepsilon_\mathrm{F}$ would make more negative the term, $q\varepsilon_\mathrm{F}$ (since $q > 0$ for any donor spontaneously formed), thereby enhancing the spontaneous formation through thermodynamics of compensating donor defects [by making more negative the heat of formation $\Delta H$ via Equation (1.34)], other things being equal. The terms involving $\mu_{\mathrm{D,H}}$ show the further dependence on (quasi-equilibrium) growth conditions, with these terms affecting essentially the solubility of, e.g., a substituent such as N on the O site of a ZnO crystal (the solubility obviously being enhanced under oxygen-deficient growth conditions).

A couple of experimental results dating from around 1999 have been reported which shed additional light on the p-ZnO dopability question. First, there is the report by Joseph *et al.*,[30] who sought to implement Yamamoto's co-doping idea using N and Ga as the p-type and n-type dopants, respectively. Some of the films obtained indeed appeared to be p-type, but only under specific conditions of growth and with an odd and excessive acceptor-concentration/hole-mobility trade-off.[30] In particular, the use as dopant of $N_2$ proved unsuccessful and use of $N_2O$ conditionally successful, depending also on the use of plasma excitation of the $N_2$ or $N_2O$ source gas {via an electron cyclotron resonance (ECR) source in this case].[30] It should be noted from GaN MBE growth that the commercially available radio frequency (RF) sources in general have proved much more successful than the ECR sources in "cracking" the $N_2$ source gas down to the desired neutral-atomic N species relative to the undesired ionized dimers. This dependence on the type of plasma source (ECR vs RF) might be critical for purposes of effecting p-type doping in ZnO with plasma-excited $N_2$ gas.

Interestingly, another experimental paper from around the same time discusses Ga and N co-dopants in ZnO films grown using both O and N radicals produced with the aid of separate RF plasma sources on the same system.[31]

This last work, which nominally set out to effect the co-doping approach of Yamamoto and Katayama-Yoshida,[27] found instead direct experimental evidence that (i) the approach can be fraught with serious problems[31] under certain circumstances; and (ii) worse, the layer nominally intended to be "p-ZnO" in fact turned out to be a layer of the spinel compound $ZnGa_2O_4$, which formed due to metallurgical reaction during growth between the ZnO and the high concentrations of Ga needed to effect the co-doping idea[27] as proposed.

Fortunately, in the years since, and especially most recently, numerous experimental groups now have reported the successful p-type doping of ZnO.[32–41] At the time of this writing, reported hole concentrations in the $\sim 10^{17}\,cm^{-3}$ range are becoming increasingly common, with occasional reports of (ostensible) holeconcentrations as high as $\sim 10^{19}\,cm^{-3}$ though the latter are often regarded with suspicion; for example, Zhao *et al.*[33] attribute such an anomalous $10^{19}\,cm^{-3}$-range hole concentration in their putative p-ZnO ultrasonic spray pyrolysis films grown on n-Si substrates to actually be a Hall-measurement misinterpretation due to the formation of a two-dimensional hole gas (2DHG) at the heterointer face between what they believe to be actually an n-ZnO film on the n-type Si substrate: band offsets and Fermi-level pinning they argue likely give rise to a 2DHG of high sheet concentration, and it is the latter which most likely is being reflected in their Hall measurements.[33]

Many of the recent p-type doping studies have embraced the co-doping Idea,[27] often involving N on an O site of ZnO as the acceptor with a column-III element such as Ga, Al, or In as the co-donor.[42–44] In a recent study, even Zr has been employed as co-donor: Pulsed-laser-deposited ZnO doped films on $Al_2O_3$ with hole concentrations as high as $5.49 \times 10^{19}\,cm^{-3}$ along with low resistivity ($0.026\,\Omega\cdot cm$) and not too poor mobility ($4.38\,cm^{-2}\,V^{-1}\,s^{-1}$) have been achieved in ZnO:(Zr,N) co-doped films.[36] Besides N, other column-V elements, putatively substituting for O in ZnO, have been attempted for p-type doping. For instance, a recent study based on RF magnetron-sputtered, P-doped ZnO films has shown that, by considering the effect of post-growth anneals in $O_2$, $N_2$, and Ar ambients, it can be inferred from the activation kinetics that the identity of the P-related acceptor in this case, giving hole concentrations ranging between $\sim 10^{16}$ and $10^{19}\,cm^{-3}$, is indeed substitutional $P_O$, and not a $P_{Zn} + 2V_{Zn}$ complex.[34]

The principal problems which remain include a generally low acceptor solubility, large ($\sim$100 meV) hole binding energy (implying poor dopant activation efficiency at room temperature), a low hole mobility with accompanying excessive mobility vs concentration trade-off (though unlike the aforementioned issues this one may not be fundamental), and long-term material instability. Indeed, metastable phenomena such as persistent photoconductivity, often with accompanying type-conversion (p-type to n-type) upon illumination being observed,[37] are not uncommon. Often, due to the wide range of ZnO material fabrication techniques (many leading to decidedly nonepitaxial films) involved in the ZnO doping studies, combined with the apparent heightened significance of surface-, and grain-boundary-interfacial states in determining measured electrical properties in ZnO specimens in comparison with more traditional semiconductor materials such as Si, GaAs, or even GaN, it is challenging to sift through the vast and increasing pool of ZnO doping studies and then to reach any consensus as to a "best" method or "best" dopant species to use. At present, no such consensus exists.

Summarizing this section, theoretically it appears possible in principle to achieve at least some level of p-type doping in ZnO but such structures appear fundamentally to be: (i) probably metastable if achieved experimentally (unless current theories are wrong); (ii) evidently achievable experimentally (though by no means is there a universal consensus as to the best dopants or methods to use); and (iii) difficult to precisely reproduce and often challenging to interpret experimental results due to the wide variability of ZnO microstructural quality and character (often nonepitaxial in recent studies), as well as the apparently very important, and yet-to-be clarified, role of defect states at the typically high density of surfaces and interfaces between grain boundaries.

### 1.4.4 Schottky Barriers and Ohmic Contacts

For any practical implementation of ZnO-related materials as a viable optoelectronic device technology, in addition to the importance of achieving control over p-ZnO will be the control over fabrication of high quality metal/semiconductor interfaces, including both ohmic contacts as well as Schottky barriers. Progress between these two are in fact interdependent since ohmic contacts ultimately will have to be developed for both n-type and p-type material layers. However, as material control of the ZnO itself improves, so also should the control and reproducibility of the metal/semiconductor interface. Indeed, control of the material quality of any metal is trivial compared with that of the semiconductor side of the interface between the two, as has been the case in the development of every technologically significant semiconductor/metal system.

Concerning Schottky barriers, virtually all work reported to date, from the pioneering work of Mead[45] in the 1960s on cleaved ZnO surfaces to the flurry of recent work[46–53] done on the best presently available (hydrothermally or pressurized-melt-grown) bulk single-crystal materials, has been on n-type ZnO due to the historical unavailability of p-type specimens. Since ZnO is a wide-gap semiconductor with significant partially ionic bonding character, one might expect[54] Schottky barrier heights on n-type material ($\varphi_{\mathrm{Bn}}$) to obey the simple Schottky–Mott model[55] that $\varphi_{\mathrm{Bn}} = \Phi_{\mathrm{M}} - \chi_{\mathrm{S}}$, where $\Phi_{\mathrm{M}}$ is the work function of the metal and $\chi_{\mathrm{S}}$ is the electron affinity of the semiconductor. Instead, most $\varphi_{\mathrm{Bn}}$ values for ZnO range from 0.6 to 0.8 eV regardless of metal used, with ideality factors near unity being more the exception than the rule.[47,48] Briefly, Schottky barriers have been examined for numerous noble metals, including Ag and Au,[56–58] Pt[59–63] and Pd,[46,64–66] as well as metals such as Ni and Ir.[48] Allen *et al.*[47] have observed that only a small fraction of the available $\varphi_{\mathrm{Bn}}$ values for these metals from the literature involve "good" ideality factors (e.g. $\leq 1.1$), with in general a wide variability in reported barrier height values for any given metal (see Figure 1.4). Part of the variability is due to surface polarity: for several metals, including Pt, Pd, and most recently[47,48] "silver oxide" (precise stoichiometry not given), substantially higher $\varphi_{\mathrm{Bn}}$ values have been observed on Zn-polar than on O-polar {0001} surfaces.[46,47] This is explained in terms of surface-polarity-dependent band bending due to the large spontaneous polarization of ZnO along its *c*-axis.[47] Another part of the variability has been attributed to such factors as lateral inhomogeneity.[46,64] This causes $\varphi_{\mathrm{Bn}}$ measured by *I–V* to be lower than that by *C–V* measurement, as well as not only a larger, but also a linearly temperature-dependent, ideality factor.[64] But the most important part of the variability appears to be due to the influence of surface or near-surface defect states.[48–50] For example, Allen and Durbin[48]

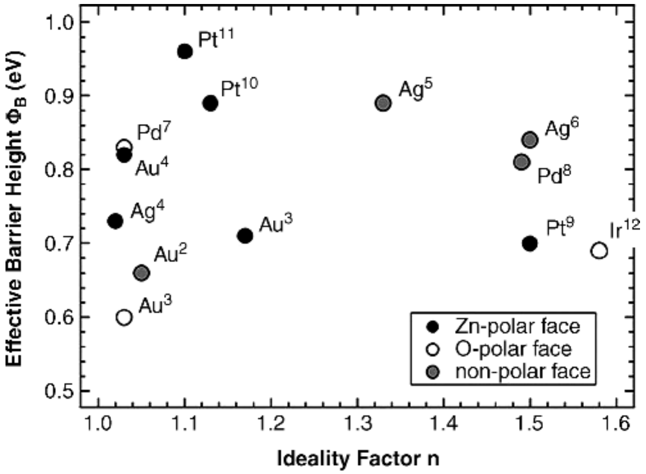

*Figure 1.4* The "best" Schottky barrier height data from the literature for several metals on n-type ZnO, from Allen et al.[47] Superscripts on element symbols correspond to the sources cited therein. Wide variability in reported $\varphi_{Bn}$ and generally large ideality factors ($\geq 1.1$) are typical; a systematic dependence on surface polarity (Zn- or O-face) is also apparent. Reprinted from M. W. Allen, S. M. Durbin, and J. B. Metson, Silver Oxide Schottky contacts on n-type ZnO. Appl. Phys. Lett. 91,053512. Copyright (2007) with permission from American Institute of Physics

have proposed that metal-induced gap states in the form of $V_O$, a known double donor with level approximately $0.7 \pm 0.2$ eV below the conduction band,[67] can form at the surface via metallurgical oxidation reaction of the metal (drawing O from the ZnO and thus forming $V_O$ levels at enhanced concentration in a thin layer near the interface). The enhanced concentration of $V_O$ deep donors thus formed serve to pin the Fermi level (thereby causing departure from the Schottky–Mott model of Schottky barrier formation) and might account for the previously mentioned 0.6–0.8 eV range barrier heights irrespective of metal species, plus poor ideality factor, often observed on ZnO. To support this hypothesis, the same authors investigated $\varphi_{Bn}$ for silver oxide (a species already reacted with oxygen thus needing no more), and found that, unusually, the silver oxide Schottky barriers exhibited an exceptionally low (for ZnO) ideality factor of 1.06. Several other authors also have noted the beneficial effect on ideality factor of pre-treating the ZnO surface prior to metallization with an oxygen-containing chemical[59] or plasma:[50] presumably, such treatment either removes adsorbates, or reduces the near-surface $V_O$, or possibly does both, with the specific phenomenological details varying from metal to metal as well as depending upon inherent material quality of the ZnO specimen itself.

Concerning ohmic contacts, investigations on both n-type[68–74] and p-type[75–77] ZnO have been performed. Generally speaking, to produce the best n-type ohmic contacts the most successful approach to date has been a multilayer metallization scheme wherein the bottom layer (i.e. the layer in direct contact with ZnO) is reactive (especially if that reaction tends to remove O from ZnO) with nominally small $\varphi_{Bn}$ to ZnO, and the top layer is a noble metal. For example, Kim *et al.* have investigated[70,72] Al/Pt contacts to n-type ($n \sim 10^{18}\,\mathrm{cm}^{-3}$) ZnO, both as deposited, and, as a function of post-metallization anneal treatment. They obtain good specific contact resistance ($\sim 1 \times 10^{-5}\,\Omega\,\mathrm{cm}^2$) even without any anneal; this they attribute to

Al/O interdiffusion resulting in the formation of a high density of near-surface $V_O$ defects which, as we noted earlier in our discussion of Schottky barriers, constitute a double donor. This effect is enhanced upon annealing to $\approx$300 °C for 1 min, whereupon the specific contact resistance decreases[72] to $\sim 2 \times 10^{-6}\,\Omega\,\text{cm}^2$. However, higher-temperature annealing (to $\approx$600 °C) is seen to be deleterious: evidently, an insulating layer of aluminum oxide compound (presumably $Al_2O_3$) forms interfacially (hence an insulator becomes interposed between semiconductor and metal layers) when the annealing time/temperature become too high, resulting in an increase (rather than a decrease) in specific contact resistance. A somewhat analogous set of phe-nomenology is found in connection with a different[73,74] metallization scheme: Ti/Al/Pt/Au. In this case, annealing beyond even $\approx$200 °C is sufficient to cause degradation.[74] Finally, additional metallization schemes have been explored. Kim *et al.*, in addition to examining Ti/Au in early work[68,69] and Al/Pt subsequently,[70,72] have most recently considered a Re/Ti/Au metallization scheme,[71] wherein the latter proved to be metallurgically stable even following a high-temperature ($\approx$700 °C, 1 min) anneal treatment as well as resulting in superior specific contact resistance of $\sim 2 \times 10^{-7}\,\Omega\,\text{cm}^2$ (for comparable ZnO doping levels) in comparison with Al/Pt.

Studies of ohmic contacts to p-type ZnO are fewer to date but are becoming increasingly reported as p-type ZnO material availability and quality steadily improve. In 2005, the same Korean group (Kim *et al.*) whose n-type ohmic contact studies were overviewed above also have looked at p-type material. In one study they employed a Ni/indium-tin-oxide scheme[76] and in the other a Ni/Au scheme.[75] In both, Ni from the metallization interdiffused and reacted metallurgically with the Zn from ZnO to form many intermetallic phases, ultimately yielding decent preliminary specific contact resistances ($\sim 10^{-4}\,\Omega\,\text{cm}^2$) in each case.[75,76] Lastly, in a separate study of Au/Ni contacts by Mandalapu *et al.*[77] involving rapid thermal annealing ($\approx$800 °C, 1 min), it was conjectured that the good specific contact resistance (again $\sim 10^{-4}\,\Omega\,\text{cm}^2$) was the result of Zn vacancies (due to Zn outdiffusion), coupled with activated Sb atoms, to increase the surface hole concentration which enables the formation of ohmic *I–V* characteristics at the metal/ZnO junction.

## 1.5 Band Gap Engineering

In this section we consider the prospects and survey the current status of attempts at band gap engineering within the (Zn,Mg,Cd)O heteroepitaxial system. In analogy with other semiconductors, the use of heterojunctions to confine carriers and/or light has played an important role in the performance optimization of modern commercial optoelectronic devices [e.g. separate-confinement heterostructure (SCH) lasers]. Additionally, tailoring the band gap permits a range of wavelength-tunability in the device design. Of particular significance given the present commercial and security interests in achieving UV-range optoelectronics is the possibility for pushing ZnO to even shorter wavelengths through alloying with larger-gap materials which are compatible with the crystal structure of ZnO so as to enable heteroepitaxial integration within a transparent-oxide II–VI ZnO-based system, in analogy to the (In,Al,Ga)N III–V system. Finally, in the event that adequate control for device requirements of p-type doping in ZnO proves too difficult to be practical (especially in the short term), a novel alternative approach might involve the direct injection of holes via an appropriate heterojunction combination with other suitably matched heterostructures including heterovalent combinations with III–V nitrides or with, as shall be described below, certain spinel compounds. A very brief look at some possibilities will be considered next.

### 1.5.1 Homovalent Heterostructures

Theoretically, the hypothetical, wurtzite-equivalent band gaps for MgO, ZnO, and CdO, all direct, are believed to correspond closely in magnitude to those of the nitrides AlN, GaN, and InN, respectively, with MgO and CdO each forming a type-I band alignment to ZnO, and with relatively smaller band offsets (as well as smaller hydrostatic deformation potentials) expected theoretically for the valence bands in comparison with the conduction band.[78] Experimentally, it is possible to enlarge the ZnO band gap through formation of wurtzite $Mg_xZn_{1-x}O$ alloys provided that $x$ is not too large. Similarly, it is possible to create ZnO based separate-confinement structures through alloying with $Cd_yZn_{1-y}O$, again, with the restriction that $y$ remain sufficiently small. Since only relatively recently has it become possible to fabricate ZnO itself of sufficient epitaxial quality to warrant extrapolation to ZnO-based heterostructures, presently there is not an extensive body of research to be found concerning ZnO-based heteroepitaxy.

The pioneering experimental work in this area has been accomplished by a group of researchers[79–81] based in Japan; this group was the first to significantly extend the compositional range of achievable (Zn,Mg,Cd)O alloys while retaining a reasonable degree of material quality.

Figure 1.5 summarizes the experimental state of affairs in terms of achievable ternary compositions, band gaps, and lattice constants involving $Mg_xZn_{1-x}O$ and $Cd_yZn_{1-y}O$, as of 2001.[81] Before we consider this figure in detail, it is important not to make too facile a comparison with the status of much more mature (and from the material-synthesis standpoint much less formidable) material systems such as Si–Ge, the III–V arsenides, phosphides, antimonides, or even the nitrides. In sharp contrast to any of the aforementioned systems, the material constraints imposed by thermodynamics within the (Zn,Mg, Cd)O system are fundamentally far more difficult to surmount. In particular, both CdO and MgO crystallize only in the NaCl (i.e. rocksalt) structure whereas ZnO exists only in wurtzite form. This basic structural incompatibility occurs in no other established heteroepitaxial system (including the nitrides). Not surprisingly, MgO–ZnO and CdO–ZnO pseudobinary systems have extremely limited miscibility: in thermodynamic equilibrium, the reported limits in alloy composition are $x \leq 4\%$ for the $Mg_xZn_{1-x}O$ ternary and $y \leq 2\%$ for the case of $Cd_yZn_{1-y}O$. Thus, nonequilibrium growth techniques will be essential to extend these limits; moreover, any structures so produced will be structurally metastable and subject to phase segregation beyond certain time and temperature limits of device processing.[80]

Returning now to Figure 1.5, despite the warning given, the results to date do bode very optimistically for extending the working wavelength range of prospective ZnO-based optoelectronics, in particular, in pushing it further into the UV. We see that, in metastable thin film form, $Mg_xZn_{1-x}O$ films grown by the pulsed laser deposition technique[81] have been grown out to $x_{\max} \approx 33\%$, corresponding to a direct band gap close to 4.0 eV. Comparable alloy compositions have since been achieved through other nonequilibrium growth techniques such as plasma-assisted molecular beam epitaxy (P-MBE).[82] Simi-

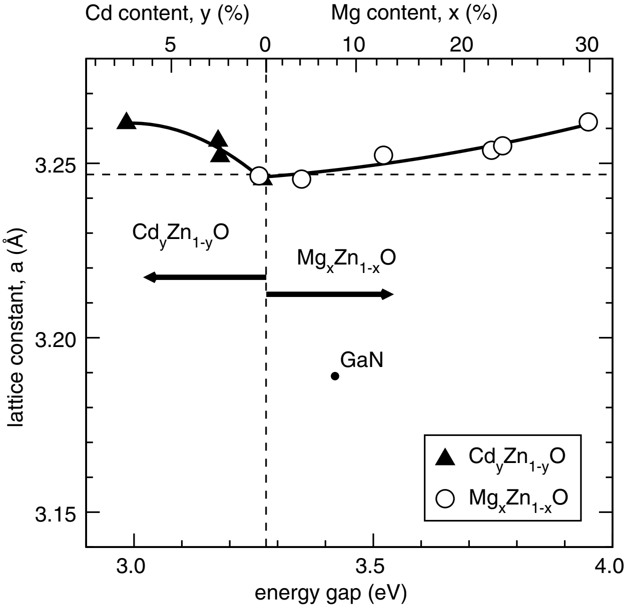

***Figure 1.5*** *Lattice constant vs band gap for $Mg_xZn_{1-x}O$ and $Cd_yZn_{1-y}O$ ternary films produced by pulsed laser deposition. Reprinted from T. Makino, et al., Band gap engineering based on $Mg_xZn_{1-x}O$ and $Cd_yZn_{1-y}O$ ternary alloy films. Appl. Phys. Lett. 78, 1237 (2001).*

larly, from the figure we also see that for $Cd_yZn_{1-y}O$ the miscibility limits are even more stringent than for $Mg_xZn_{1-x}O$ (metastable $y_{\max} \approx 7\%$), even in epitaxial form, with the minimum Band gap (at the most Cd-rich concentration) occurring near 3.0 eV. Fortunately, the compositional range of metastable wurtzite $Cd_yZn_{1-y}O$ films has since been extended substantially, with $y_{\max} \approx 69\%$, corresponding to band gaps as small as ≈1.8 eV, through the use of nonequilibrium growth techniques such as remote plasma-enhanced metal organic chemical vapor deposition (RPE-MOCVD) which, owing to the use of plasma excitation, enables epitaxial growth at unusually low substrate temperatures (325–400 °C) as needed for the formation of the metastable films.[83]

Recent theoretical studies tend to support the above experimental findings. An *ab initio* study of relative thermodynamic stabilities for rocksalt vs wurtzite $Mg_xZn_{1-x}O$ alloy hypothetical single crystals by Fan *et al.*[84] has confirmed the oretically, upon comparing formation enthalpies as the basis for assessing relative thermodynamic stability, that the wurtzite phase remains more stable than the rocksalt phase for sufficiently low Mg content ($x \leq 37\%$). (Of course, this assessment merely concerns the relative stability of two metastable forms: fundamentally, neither wurtzite nor rocksalt $Mg_xZn_{1-x}O$ are stable with respect to spontaneous phase segregation into a ZnO + MgO mixture, consistent with the experimentally well known 4% solubility limit for MgO in ZnO mentioned earlier.) Similarly, at high Mg concentration ($x \geq 50\%$), rocksalt theoretically is more stable than wurtzite.[84] These predictions conform nicely to the empirical observations that metastable $Mg_xZn_{1-x}O$ layers grown with $x \leq 33\%$ are found to consist of uniform wurtzite films whereas those at high concentrations (over 65%) are found to be uniform rocksalt films, with films of intermediate composition yielding a wurtzite–rocksalt mixture.[82] The same *ab initio* study[82] also considered $Cd_yZn_{1-y}O$ and reached analogous conclusions; theoretical results once are again consistent with experiment. Specifically, wurtzite should be favored over rocksalt structure for Cd content all the way up to $y \approx 70\%$.[82]

### 1.5.2 Heterovalent Heterostructures

An interesting way to circumvent the ZnO p-type dopability problem might be to form a heterojunction with a material which can be doped p-type readily, and then to devise a device structure which allows the ZnO layer to function as an n-type active layer in the overall structure. An early step in this direction was reported by Ohta *et al.*,[85] who fabricated and demonstrated successfully a working p-n light-emitting diode (LED) structure involving the heterojunction combination: p-$SrCu_2O_2$/n-ZnO. For this device a hard rectifying *I–V* diode characteristic was obtained with turn-on at 3 V and a prominent electroluminesence (EL) peak at 382 nm which the authors attributed to electron–hole plasma recombination in ZnO.[85] Both the electrical and spectral characteristics for this heterojunction LED appear superior to those of a homojunction ZnO LED (epitaxial p-ZnO on a n-ZnO substrate) reported by Aoki *et al.*[86] which resulted in a softer and leakier *I–V* characteristic as well as an EL spectrum which was much broader and noisier despite a strong, band-gap-dominated photoluminescence (PL) spectrum. Possibly, the different outcomes are in part due to the fact that only for the heterojunction device were all of the active layers entirely epitaxial.[85,86]

Since these earliest device attempts, much additional work on heterovalent heterostructures has been undertaken. To date, the following structures, each involving an n-type-ZnO layer in combination with a p-type non-II–VI material, have been re ported: n-ZnO/p-$SrCu_2O_2$ (already mentioned above);[85] n-ZnO/p-GaN;[87] n-ZnO/p-$Al_xGa_{1-x}N$;[88] n-ZnO/p-SiC;[89] as well as even more exotic heterostructural combinations such as n-$Mg_xZn_{1-x}O$/n-ZnO/p-$Al_xGa_{1-x}N$/p-GaN.[90] In 2007, "full-color electroluminescence" LEDs were reported, with individual RGB pixel color determined by the Cd content of a $Cd_yZn_{1-y}O$ quantum well (with $y = 7\%$, 17%, and 58% for blue, green, and red emission at room temperature, respectively).[91] In this device, the appropriate quantum well was sandwiched between a p-type-SiC layer (substrate) and an n-$Mg_{0.04}Zn_{0.96}O$ barrier layer with a capping layer of n-ZnO.[91] Overall, the device results look encouraging for electrically injected UV ZnO-based emitters but also demonstrate that achieving good electrically injected UV emission will be considerably more challenging than merely achieving good optically-pumped emission in ZnO-based materials.

## 1.6 Spintronics

ZnO-based dilute magnetic semiconductors can be manipulated in these low-dimensional tailored thin films for various spin-based devices to unprecedented capabilities.[92,93] In these materials, the transition metal ions are substitutional on the cation sites of ZnO, giving (Zn,TM) O. In modeling these interactions, one can use the Heisenberg Spin Hamiltonian given by

$$\mathcal{H}_{\text{eff}} = \text{const.} - 2\sum_{i<j} J_{ij}\hat{S}_i \cdot \hat{S}_j \tag{1.35}$$

where $J_{ij}$ is the exchange term and $\hat{S}_i$ is the spin generator. There are two cases of exchange interactions: (1) the d–d superexchange between d electrons of the magnetic ions; and (2) the sp–d exchange between the d electrons and the band electrons or holes. In general this interaction is antiferromagnetic for conduction band states and ferromagnetic for valence band states. One can use the Curie–Weiss law to obtain the Curie temperature, $T_C$, from the magnetic measurements:

$$\frac{M}{H} = \frac{C_0 x}{T - \Theta_0 x} \tag{1.36}$$

where $M$ is the magnetization, $H$ is the magnetic field, $T$ is the temperature, $x$ is the transition metal composition, and $\Theta_0$ and $C_0$ are the Curie–Weiss temperature and the Curie constant for $x = 1$, respectively. The Curie constant is expressed as[94]

$$C_0 = \frac{(g\mu_B)^2 S(S+1)_n}{3k_B} = C_n \rho/\mu \tag{1.37}$$

where $g$ is the intrinsic Landé $g$ factor, $n$ is the number of cation sites per unit volume, $C_n$ is the Curie constant for $x = 1$, $\rho$ is the mass density, $\mu$ is the molar mass, $S$ is the effective spin per TM ion ($S = 5/2$ for $n = 2$), $\mu_B$ is the Bohr magneton and $k_B$ is the Boltzmann constant. Using Equations (1.35) and (1.36) one can estimate $\Theta_0$ and $C_n$. The effective exchange integral between the nearest-neighbor transition ions can be estimated from

$$\frac{J_1}{k_B} = \frac{3\Theta_0}{2zS(S+1)} \tag{1.38}$$

where $z$ equals the number of nearest neighbors; $z = 12$ for the wurtzite lattice. A negative value of $J_1$ indicates that the interactions between the magnetic ions are antiferromagnetic, suggesting that superexchange is likely to be the dominant mechanism.

For an external magnetic field $B$ applied along the $z$-axis direction, the magnetization $M_z$ of the dilute magnetic semiconductor (DMS) alloy containing $Mn^{2+}$ ions is empirically written as

$$M_z = (N_0\langle S_x \rangle) + N_0 S_{\mathrm{sat}} B_{5/2}(5\mu_B B/k_B T_{\mathrm{eff}}) \tag{1.39}$$

where $N_0$ is the density of $Mn^{2+}$ ions and $B_{5/2}(x)$ is the Brillouin function for $S = 5/2$, $S_{\mathrm{sat}}$ is the saturation value for the spin of the individual $Mn^{2+}$ ions and the rescaled temperature is $T_{\mathrm{eff}} = T + T_0$. Along with the distribution of magnetic ions on a DMS lattice, isolated spins, pairs of spins, and triplets are distributed; hence, the magnetization is dominated by the paramagnetic response of isolated single spins, which are antiferromagnetically coupled. However, if a DMS heterostructure is considered, the ferromagnetic sp–d exchange interaction between conduction electrons and local moments results in the enhanced electromagnetic spin splitting as

$$\Delta E = g\mu_B B + f(\psi)(N_0\alpha)\langle S_z \rangle \tag{1.40}$$

where $f(\psi)$ is the wave function overlap between the combined and local moments and $\alpha$ is the sp–d exchange integral. The spin splitting is dominated by the second term in

Equation (1.40) because the intrinsic $g$ factor for electrons in ZnO is small.[95] The exchange integral for the heavy-hole states is ~5 times larger than that for the conduction band and light hole states. For this reason, the spin splitting is dominated by that of the valence band states.

Progress toward understanding the (Zn,TM)O band materials and, in particular, the mechanism limiting the Curie temperature, $T_C$, requires careful investigation of the transport behavior; that is, it requires precise knowledge of the hole density $p$. The Hall resistivity in magnetic materials is given by

$$\rho_{xy} = \rho_{xy}^{0} + \rho_{xy}^{\alpha} = R_0 B + R_\alpha(\rho_{xy})M \tag{1.41}$$

where the normal contribution $\rho_{xy}^{0}$ is proportional to the external magnetic field $B$, $R_0 = 1/pe$ and the anomalous contribution $\rho_{xy}^{\alpha}$ is proportional to the macro-scopic magnetization $M$. The term $R_\alpha$ arises from the spin-orbit interaction, which include anisotropy between scattering of spin-up and spin-down electrons. The Hall measurements should be carried out in the applied magnetic field limit where magnetization is saturated (low $T$ and high $H$).

In dilute magnetic systems, ferromagnetism has been accounted for by the formation of bound magnetic polarons.[95–103] The bound magnetic polarons are formed by alignment of the spins of the transition metal ions with that of a much lower number of weakly bound carriers such as excitons within a polariton radius. The localized holes of the polarons interact with the TM impurity surrounding them, thus producing an effective magnetic field and aligning the spins. The interaction distance grows with decreasing temperature. Neighboring magnetic polarons overlap and interact via magnetic impurities forming correlated clusters of polarons. One has a ferromagnetic transition when the size of such clusters is equal to the size of the sample. This model is inherently attractive for low-carrier-density systems such as many of the electronic oxides. The polaron model is applicable to both p-type and n-type materials.[99] Even though the direct exchange interaction of the localized holes is antiferromagnetic, the interaction between bound magnetic polarons may be ferromagnetic for large concentrations of magnetic impurities. This enables ferromagnetic ordering of the $Mn^{2+}$ ions in an otherwise insulating or semi-insulating material.

Dietl *et al.* [104] and Dietl[105] evaluated the Curie temperature for ZnO. The short bond length leads to a strong coupling between holes (on anions) and the spin of the transition metal ions on the Zn site. They showed that the holes in the extended or weakly bound states mediate the long-range interactions between the localized spins on both sides of the metal–insulator transition. This allows the use of the mean-field approximation, giving that a competition exists between the ferromagnetic and antiferromagnetic interactions. The $T_C$ is proportional to the density of the $Mn^{2+}$ ions and the hole density.

The theory by Dietl *et al.*[104] assumes that ferromagnetic correlations among the $Mn^{2+}$ ions, which provide the spin, are mediated by the holes from the shallow acceptors. This model suggests that the carrier-mediated ferromagnetism in n-type materials may be observed only at low temperature with shallow donors while high temperatures for p-type materials with $T_C > 300\,K$ are predicted for ZnO.

## 1.7 Summary

In this chapter, we have reviewed aspects of the fundamental electronic band structure and electrical characteristics of intrinsic and doped ZnO as well as having surveyed recent important theoretical and experimental developments which, taken together, bode encouragingly for the future of epitaxial ZnO for eventual utilization as a UV-range optoelectronic device material. While ZnO in poly-crystalline form has enjoyed diverse technological use for decades, only now, through the advent of modern nonequilibrium crystal-growth techniques, combined with recent key theoretical advances (especially as concerns the long-standing p-type dopability question) does the promise, long held, of efficient UV-range epitaxial-ZnO-based optoelectronics finally appear to be reachable. As we have described, the principal inherent advantage of ZnO–in relation to other comparably wide-gap UV-range semiconductors–is the exceptionally deep exciton binding energy: at 60 meV, the binding energy of ZnO is three times that of rival GaN and fundamentally provides a highly efficient excitonic recombination mechanism which dominates at room temperature and even above. Within only the past decade, remarkable progress has been made in key areas, all essential to realizing the promise of using ZnO as the active layers of epitaxial devices. These include: quality improvement of bulk ZnO (substrate material), experimental demonstration of p-type doping, successes in the synthesis of heteroepitaxial (Mg,Cd,Zn)O metastable material combinations, and reports of significant progress in the fabrication of ohmic and Schottky contacts to ZnO. The advantage to the quality of epitaxy through having available a homoepitaxial substrate (which is lacking for GaN) cannot be underestimated. To date, numerous demonstrations of electrically injected ZnO-based LED devices have been made, with preliminary reports of electrically injected stimulated emission now beginning to appear, showing directly that, despite the long developmental road which lies ahead (which hopefully will be shortened some-what through lessons learned from the nitrides) that the future shines brightly for ZnO. Finally, over the last four years, thanks to a Curie temperature above room temperature, the potential use of ZnO in spintronics applications appears particularly promising.

## References

[1] D. C. Reynolds and T. C. Collins, *Excitons, Their Properties and Uses*, Academic Press, New York, 1981, p. 29.
[2] M. Belkanski and J. des Cloizeaux, *J. Phys. Radium* **21**, 825 (1960).
[3] S. Adler and J. L. Birman, *Gen. Teleph. Electron. Corp. Res. Dev. J.* **1**, 2 (1961).
[4] J. J. Hopfield, *J. Phys. Chem. Solids* **15**, 97 (1960).
[5] D. G. Thomas, *J. Phys. Chem. Solids* **15**, 86 (1960).
[6] M. Cardona, *Phys. Rev.* **129**, 69 (1963).
[7] C. J. Vasely, R. L. Hengehold and D. W. Langer, *Phys. Rev.* **35**, 2296 (1972).
[8] R. A. Powell, W. E. Spicer and J. C. McMenamin, in *Electron Spectroscopy*, edited by D. A. Shirley, North-Holland, Amsterdam, 1972, p. 575.
[9] S. K. Hong, T. Hanada, H. Makino, H.-J. Ko, Y. Chen, T. Yao, A. Tankaka, H. Sasaki, S. Sato, D. Imai, K. Araki and M. Shinohara, *J. Vac. Sci. Technol. B* **19**, 1429 (2001).

[10] D. C. Reynolds, D. C. Look, B. Jogai, C. W. Litton, G. Cantwell and W. C. Harsch, *Phys. Rev. B* **60**, 2340 (1999).

[11] W. R. L. Lambrecht, A. V. Rodina, S. Lumpijumnong, B. Segall and B. K. Meyer, *Phys. Rev. B* **65**, 075207 (2002).

[12] R. G. Wheeler and J. O. Dimmock, *Phys. Rev.* **125**, 1805 (1962).

[13] G. E. Pikus, *Fiz. Tverd. Tela* **6**, 324 (1964) [ *Sov. Phys. Solid State* **6**, 324 (1964) ]

[14] D. W. Langer, R. N. Euwena, K. Era and T. Koda, *Phys. Rev. B* **2**, 4005 (1970).

[15] Landolt-Börnstein, *Physics of II-VI and I-VII Compounds, Semimagnetic Semiconductors*, edited by O. Madelung, Springer, New York, 1982, Group III, Vol. 17b

[16] H. Sheng, S. Mulhukumar, N.W. Emanetogler, and Y. Lu, *Appl. Phys. Lett.* **80**, 2132 (2002).

[17] T. Minami, H. Sato, H. Nanto and S. Takata, *Jpn. J. Appl. Phys.* **24**, L781 (1985).

[18] S. B. Zhang, S.-H. Wei and A. Zunger, *Phys. Rev. B* **63**, 75 205 (2001).

[19] E.-C. Lee, Y.-S. Kim, Y.-G. Jin and K. J. Chang, *Phys. Rev. B* **64**, 085120 (2001).

[20] C. G. Van de Walle, *Phys. Rev. Lett.* **85**, 1012 (2000).

[21] R. Helbig and P. Wagner, *J. Phys. Chem. Solids* **35**, 327 (1974).

[22] J. D. Albrecht, P. P. Ruden, S. Limpijumnong and W. R. L. Lambrecht, *J. Appl. Phys.* **86**, 6864 (1999).

[23] D. C. Look, *Mater. Sci. Eng., B* **80**, 383 (2001).

[24] D. C. Look, J. W. Hemsky, J. R. Sizelove, Phys. Rev. Lett. **82**, 2552 (1999).

[25] U. V. Desnica, *Prog. Cryst. Growth Charact.* **36**, 291 (1998).

[26] K. Minegishi, Y. Koiwai, Y. Kikuchi, K. Yano, M. Kasuga and A. Shimizu, *Jpn. J. Appl. Phys.* **36**, L1453 (1997) and references therein.

[27] T. Yamamoto and H. Katayama-Yoshida, *Jpn. J. Appl. Phys.* **38**, L166 (1999).

[28] Y. Yan, S. B. Zhang and S. T. Pantelides, *Phys. Rev. Lett.* **86**, 5723 (2001).

[29] A. Zunger, *Appl. Phys. Lett.* **83**, 57 (2003).

[30] M. Joseph, H. Tabata and T. Kawai, *Jpn. J. Appl. Phys.* **38**, L1205 (1999).

[31] K. Nakahara, H. Takasu, P. Fons, A. Yamada, K. Iwata, K. Matsubara, R. Hunter and S. Niki, *Appl. Phys. Lett.* **79**, 4139 (2001).

[32] H. B. Ye, J. F. Kong, W. Z. Shen, J. L. Zhao and X. M. Li, *Appl. Phys. Lett.* **90**, 102115 (2007).

[33] J. L. Zhao, X. M. Li, A. Krtschil, A. Krost, W. D. Yu, Y. W. Zhang, Y. F. Gu, and X. D. Gao, *Appl. Phys. Lett.* **90**, 062118 (2007).

[34] D. K. Hwang, M. S. Oh, J. H. Lim, C. G. Kang and S. J. Park, *Appl. Phys. Lett.* **90**, 021106 (2007).

[35] W. Guo, A. Allenic, Y. B. Chen, X. Q. Pan, Y. Che, Z. D. Hu and B. Liu, *Appl. Phys. Lett.* **90**, 242108 (2007).

[36] H. Kim, A. Cepler, M. S. Osofsky, R. C. Y. Auyeung and A. Pique, *Appl. Phys. Lett.* **90**, 203508 (2007).

[37] Z. Y. Xiao, Y. C. Liu, R. Mu, D. X. Zhao and J. Y. Zhang, *Appl. Phys. Lett.* **92**, 052106 (2008).

[38] X. H. Pan, J. Jiang, Y. J. Zeng, H. P. He, L. P. Zhu, Z. Z. Ye, B. H. Zhao and X. Q. Pan, *J. Appl. Phys.* **103**, 023708 (2008).

[39] S. T. Tan, X. W. Sun, Z. G. Yu, P. Wu, G. Q. Lo and D. L. Kwong, *Appl. Phys. Lett.* **91**, 072101 (2007).

[40] B. J. Kwon, H. S. Kwack, S. K. Lee, Y. H. Cho, D. K. Hwang and S. J. Park, *Appl. Phys. Lett.* **91**, 061903 (2007).

[41] Z.-Q. Fang, B. Claflin, D. C. Look, L. L. Kerr and X. Li, *J. Appl. Phys.* **102**, 023714 (2007).

[42] M. Kumar, T.-H. Kim, S.-S. Kim and B.-T. Lee, *Appl. Phys. Lett.* **89**, 112103 (2006).

[43] G. D. Yuan, Z. Z. Ye, L. P. Zhu, Q. Qian, B. H. Zhao, R. X. Fan, C. L. Perkins and S. B. Zhang, *Appl. Phys. Lett.* **86**, 202106 (2005).

[44] L. L. Chen, J. G. Lu, Z. Z. Ye, Y. M. Lin, B. H. Zhao, Y. M. Ye, J. S. Li and L. P. Zhu, *Appl. Phys. Lett.* **87**, 252106 (2005).

[45] C. A. Mead, *Solid-State Electron.* **9**, 1023 (1966).

[46] M. W. Allen, M. M. Alkaisi and S. M. Durbin, *Appl. Phys. Lett.* **89**, 103520 (2006).

[47] M. W. Allen, S. M. Durbin, and J. B. Metson, *Appl. Phys. Lett.* **91**, 053512 (2007).

[48] M. W. Allen and S. M. Durbin, *Appl. Phys. Lett.* **92**, 122110 (2008).

[49] L. J. Brillson, H. L. Mosbacker, M. J. Hetzer, Y. Strzhemechny, G. H. Jessen, D. C. Look, G. Cantwell, J. Zhang and J. J. Song, *Appl. Phys. Lett.* **90**, 102116 (2007).

[50] H. L. Mosbacker, S. El Hage, M. Gonzalez, S. A. Ringel, M. Hetzer, D. C. Look, G. Cantwell, J. Zhang, J. J. Song and L. J. Brillson, *J. Vac. Sci. Technol. B* **25**, 1405 (2007).

[51] M. Nakano, A. Tsukazaki, R. Y. Gunji, K. Ueno, A. Ohtomo, T. Fukumura and M. Kawasaki, *Appl. Phys. Lett.* **91**, 142113 (2007).

[52] M.-S. Oh, D.-K. Hwang, J.-H. Lim, Y.-S. Choi and S.-J. Park, *Appl. Phys. Lett.* **91**, 042109 (2007).

[53] R.Y. Gunji, M. Nakano, A. Tsukazaki, A. Ohtomo, T. Fukumura and M. Kawasaki, *Appl. Phys. Lett.* **93**, 012104 (2008).

[54] S. Kurtin, T.C. Mcgill, and C.A. Mead, *Phys. Rev. Lett* **22**, 1433 (1969).

[55] W. Schottky, *Naturwissenschaften* **26**, 843 (1938); N. F. Mott, *Proc. Cambridge Philos. Soc.* **34**, 568 (1938).

[56] A. Y. Polyakov, N. B. Smirnov, E. A. Knozhukhova, V. I. Vdovin, K. Ip, D. P. Norton and S. J. Pearton, *J. Vac. Sci. Technol. A* **21**, 1603 (2003).

[57] A. Y. Polyakov, N. B. Smirnov, E. A. Knozhukhova, V. I. Vdovin, K. Ip, Y. W. Heo, D. P. Norton and S. J. Pearton, *Appl. Phys. Lett.* **83**, 1575 (2003).

[58] D. C. Oh, J. J. Kim, H. Makino, T. Hanada, M. W. Cho, T. Yao and H. J. Ko, *Appl. Phys. Lett.* **86**, 042110 (2005).

[59] S.-H. Kim, H.-K. Kim and T.-Y. Seong, *Appl. Phys. Lett.* **86**, 112101 (2005).

[60] S. Kim, B. S. Kang, F. Ren, K. Ip, Y. W. Heo, D. P. Norton and S. J. Pearton, *Appl. Phys. Lett.* **84**, 1698 (2004).

[61] K. Ip, B. P. Gila, A. H. Onstine, E. S. Lambers, Y. W. Heo, K. H. Baik, D. P. Norton, S. J. Pearton, S. Kim, J. R. LaRoche and F. Ren, *Appl. Phys. Lett.* **84**, 5133 (2004).

[62] K. Ip, Y. W. Heo, K. H. Baik, D. P. Norton, S. J. Pearton, S. Kim, J. R. LaRoche and F. Ren, *Appl. Phys. Lett.* **84**, 2835 (2004).

[63] S.-H. Kim, H.-K. Kim and T.-Y. Seong, *Appl. Phys. Lett.* **86**, 022101 (2005).

[64] H. von Wenckstern, G. Biehne, R. A. Rahman, H. Hochmuth, M. Lorenz and M. Grundmann, *Appl. Phys. Lett.* **88**, 092102 (2006).

[65] U. Grossner, S. Gabrielsen, T. M. Borseth, J. Grillenberger, A. Yu. Kuznetsov and B. G. Svensson, *Appl. Phys. Lett.* **85**, 2259 (2004).

[66] R. Schifano, E. V. Monakhov, U. Grossner and B. G. Svensson, *Appl. Phys. Lett.* **91**, 193507 (2007).

[67] A. Janotti and C. G. Van de Walle, *Appl. Phys. Lett.* **87**, 122102 (2005).

[68] H.-K. Kim, S.-H. Han, T.-Y. Seong and W.-K. Choi, *Appl. Phys. Lett.* **77**, 1647 (2000).

[69] J.-M. Lee, K.-K. Kim, S.-J. Park and W.-K. Choi, *Appl. Phys. Lett.* **78**, 3842 (2001).

[70] H.-K. Kim, K.-K. Kim, S.-J. Park, T.-Y. Seong and I. Adesida, *J. Appl. Phys.* **94**, 4225 (2003).

[71] S.-H. Kim, K.-K. Kim, S.-J. Park and T.-Y. Seong, *J. Electrochem. Soc.* **152**, G169 (2005).

[72] H.-K. Kim, I. Adesida, K.-K. Kim, S.-J. Park and T.-Y. Seong, *J. Electrochem. Soc.* **151**, G223 (2004).

[73] K. Ip, Y. W. Heo, K. H. Baik, D. P. Norton and S. J. Pearton, *J. Vac. Sci. Technol. B* **22**, 171 (2004).

[74] K. Ip, Y. W. Heo, K. H. Baik, D. P. Norton and S. J. Pearton, *Appl. Phys. Lett.* **84**, 544 (2004).

[75] J.-H. Lim, K.-K. Kim, D.-K. Hwang, H.-S. Kim, J.-Y. Oh and S.-J. Park, *J. Electrochem. Soc.* **152**, G179 (2005).

[76] S.-H. Kang, D.-K. Hwang and S.-J. Park, *Appl. Phys. Lett.* **86**, 211902 (2005).

[77] L. J. Mandalapu, Z. Yang and J. L. Liu, *Appl. Phys. Lett.* **90**, 252103 (2007).

[78] A. Janotti and C. G. Van de Walle, *Phys. Rev. B* **75**, 121201 (2007).

[79] A. Ohtomo, M. Kawasaki, T. Koida, K. Masubuchi, H. Koinuma, Y. Sakurai, Y. Yoshida, T. Yasuda and Y. Segawa, *Appl. Phys. Lett.* **72**, 2466 (1998).

[80] A. Ohtomo, R. Shiroki, I. Ohkubo, H. Koinuma and M. Kawasaki, *Appl. Phys. Lett.* **75**, 4088 (1999).

[81] T. Makino, Y. Segawa, M. Kawasaki, A. Ohtomo, R. Shiroki, K. Tamura, T. Yasuda and H. Koinuma, *Appl. Phys. Lett.* **78**, 1237 (2001).

[82] Z. Vashaei, T. Minegishi, H. Suzuki, T. Hanada, M. W. Cho, T. Yao and A. Setiawan, *J. Appl. Phys.* **98**, 054911 (2005).

[83] J. Ishihara, A. Nakamura, S. Sigemori, T. Aoki and J. Temmyo, *Appl. Phys. Lett.* **89**, 091914 (2006).

[84] X. F. Fan, H. D. Sun, Z. X. Shen, J.-L. Kuo and Y. M. Lu, *J. Condens. Matter* **20**, 235221 (2008).

[85] H. Ohta, K. Kawamura, M. Orita, M. Hirano, N. Sarukura and H. Hosono, *Appl. Phys. Lett.* **77**, 475 (2000).

[86] T. Aoki, Y. Hatanaka and D. C. Look, *Appl. Phys. Lett.* **76**, 3257 (2000).

[87] R. W. Chuang, R.-X. Wu, L.-W. Lai and G.-T. Lee, *Appl. Phys. Lett.* **91**, 231113 (2007).

[88] Ya. I. Alivov, E. V. Kalinina, A. E. Cherenkov, D. C. Look, B. M. Ataev, A. K. Omaev, M. V. Chukichev and D. M. Bagnall, *Appl. Phys. Lett.* **83**, 4719 (2003).

[89] D. J. Rogers, F. Hosseini Teherani, A. Yasan, K. Minder, P. Kung and M. Razeghi, *Appl. Phys. Lett.* **88**, 141918 (2006).

[90] A. Osinsky, J. W. Dong, M. Z. Kauser, B. Hertog, A. M. Dabiran, P. P. Chow, S. J. Pearton, O. Lopatiuk and L. Chernyak, *Appl. Phys. Lett.* **85**, 4272 (2004).

[91] A. Nakamura, T. Ohashi, K. Yamamoto, J. Ishihara, T. Aoki, J. Temmyo and H. Gotoh, *Appl. Phys. Lett.* **90**, 093512 (2007).

[92] Ü. Özgür, Ya. I. Alivov, C. Liu, A. Teke, M. A. Reshchikov, S. Doğan, V. Avrutin, S.-J. Cho, and H. Morkoç, *J. Appl. Phys.* **98**, 041301 (2005).

[93] C. Weisbuch and B. Vinter, *Quantum Semiconductor Structures*, Academic Press, San Diego, 1991.

[94] T. Fukumura, Z. Jin, M. Kawasaki, T. Shono, T. Hasegawa, S. Koshihara and H. Koinuma, *Appl. Phys. Lett.* **78**, 958 (2001).

[95] K. Ando, H. Saito, Zhengwu Jin, T. Fukumura, M. Kawasaki, Y. Matsumoto and H. Koinuma, *J. Appl. Phys.* **89**, 7284 (2001).

[96] M. Berciu and R. N. Bhatt, *Phys. Rev. Lett.* **87**, 129702 (2001).

[97] A. Kaminski and S. Das Sarma, *Phys. Rev. B* **68**, 235210 (2003).

[98] T. Dietl, F. Matsukura and H. Ohno, *Phys. Rev. B* **66**, 033203 (2002).

[99] S. Das Sarma, E. H. Hwang and A. Kaminski, *Phys. Rev. B* **67**, 155201 (2003).

[100] J. Warnock and P. A. Wolff, *Phys. Rev. B* **31**, 6579 (1985).

[101] M. Sawicki, T. Dietl, J. Kossut, J. Igalson, T. Wojtowicz and W. Plesiewicz, *Phys. Rev. Lett.* **56**, 508 (1986).

[102] J. M. D. Coey, M. Venkatesan and C. B. Fitzgerald, *Nat. Mater.* **4**, 73 (2005).

[103] T. Dietl and J. Spałek, *Phys. Rev. Lett.* **48**, 355 (1982).

[104] T. Dietl, H. Ohno, F. Matsukura, J. Cibert and D. Ferrand, *Science* **287**, 1019 (2000).

[105] T. Dietl, *Nat. Mater.* **2**, 646 (2003).